



**HAL**  
open science

## Damage modelling of carbon/epoxy laminated composites under static and fatigue loads

Juliette Payan, Christian Hochard

► **To cite this version:**

Juliette Payan, Christian Hochard. Damage modelling of carbon/epoxy laminated composites under static and fatigue loads. *International Journal of Fatigue*, 2002, 24 (2-4), pp.299-306. 10.1016/S0142-1123(01)00085-8 . hal-00166445

**HAL Id: hal-00166445**

**<https://hal.science/hal-00166445v1>**

Submitted on 19 Dec 2024

**HAL** is a multi-disciplinary open access archive for the deposit and dissemination of scientific research documents, whether they are published or not. The documents may come from teaching and research institutions in France or abroad, or from public or private research centers.

L'archive ouverte pluridisciplinaire **HAL**, est destinée au dépôt et à la diffusion de documents scientifiques de niveau recherche, publiés ou non, émanant des établissements d'enseignement et de recherche français ou étrangers, des laboratoires publics ou privés.

# Damage modelling of laminated carbon/epoxy composites under static and fatigue loadings

J. Payan\*, C. Hochard

LMA, CNRS, 31 chemin Joseph Aiguier, 13402 Marseille Cedex 20, France

This study deals with the modelling of the behaviour of laminated carbon/epoxy composites under static and fatigue loading. The non-linear cumulative damage model developed is written on the scale of the plies. It is based on a multi-criterion approach: brittle behaviour in the fibre direction, elastoplastic damage behaviour under shear and transverse tension stress, and elastoplastic behaviour under transverse compression loading. The range of validity of the model described here is limited to the first intra-laminar macro-crack, and it does not account for the delamination processes. This first-ply failure criteria model provides a conservative approach, which should be useful in some industrial context where the highest safety is required. Static tests results obtained on plate samples are presented  $[\pm 45^\circ]_{3s}$  and hybrid glass/carbon  $[0,90]_s$  are presented: they justify the modelling adopted here. The first tension/tension fatigue test results obtained on plate samples  $[\pm 45^\circ]_{3s}$  are presented: they are used to identify the parameters of the model contributing to the shear behaviour.

*Keywords:* Composite; Laminate; Fatigue; Damage; Failure

## 1. Introduction

Modelling laminated composites undergoing damage and rupture is a complex procedure because of the large number of mechanisms (matrix micro-cracking, fibre/matrix debonding, transverse rupture, fibre rupture, delamination, etc.) involved under both static and cyclic loading conditions [1,2]. The various failure mechanisms can be described on different scales (on the laminate scale, ply scale, fibre/matrix scale, etc.) with models of different kinds [3] (rupture criteria, damage mechanics, crack density models, etc.). The fatigue life and the residual strength can be predicted by laws obtained from the experimental S-N curves [4,5] or after a computation based on the development of the damage up to the occurrence of rupture [6]. These cumulative damage models which describe the decrease in the stiffness of the material can be used to make structural computations.

In this paper, we present a non-linear cumulative damage model, which makes it possible to describe the development of damage under both static and fatigue loadings. This model is based on the models previously

proposed by Ladevèze et al. [7]. The damage mechanics is used here to describe the material on the scale of the plies, which thus makes it possible to compute any stacking sequences of the laminate. The development of the damage depends on the static and cyclic loads as well as the level of damage involved. The delamination phenomena are not accounted for in the model, which is therefore relevant only to some particular structures (tubes, for example) and laminates that are not subjected to delamination.

One of the most original points to emerge from this study is that the range of validity of the model described depends on the 'diffuse damage' phase (which is associated with micro-cracks) and is limited to the first intra-laminar macro-crack. In this respect, the modelling procedure adopted differs from the approaches in which these intra-laminar macro-cracks are integrated into the 'average' or 'homogenised' behaviour of the ply [7-9]. Here the first macro-crack is not integrated into the local behaviour of the ply for several reasons:

1. In some industrial contexts, where security is required, it is important to be able to detect the onset of macro-cracks, after which the complete failure of the laminate will probably occur. The endurance limit below which the structure will not be liable to failure

---

\* Corresponding author. Fax: +33-4-91-11-38-38.  
E-mail address: payan@lma.cnrs-mrs.fr (J. Payan).

probably corresponds to a ‘diffuse damage’ associated with micro-cracks;

2. If the size of this crack is correlated with the ply thickness in the normal direction of the plate, it will propagate almost instantaneously over a large length in the plan of the plate (i.e., it will become several tens of times greater in length than the ply thickness). With models integrating these macro-cracks and describing the ‘average’ ply behaviour, it is not possible to exactly account for the emergence or to specify the dimensions of these cracks;
3. These macro-cracks can result in other degradation phenomena, such as delamination. The behaviour of the structure can be simulated up to the occurrence of macro-cracks within the framework of the laminate theory. Accounting for the delamination, which is a 3D phenomenon and can be initiated on the edges of the plate or even inside the laminate after intra-laminar rupture, requires much heavier and more complex modelling procedures.

The first-ply failure criterion adopted here provides a conservative approach that is useful when safety is the most important constraint or eventually in the preliminary stages of composite structure design [10].

Static tests results obtained on plate samples  $[\pm 45^\circ]_{3s}$  and hybrid glass/carbon  $[0,90]_s$  are presented: they justify the modelling adopted here and the first tension-tension fatigue test results on plate samples  $[\pm 45^\circ]_{3s}$  are presented here. They were used to identify the parameters of the model contributing to the shear behaviour.

## 2. Testing under static and fatigue loadings

### 2.1. Experimental conditions

This study relates to unidirectional carbon epoxy composites. All the experiments carried out here focused on the shearing damage alone except static tests on transverse tension behaviour.

For shearing, the model coefficients were identified experimentally on machined plate samples in a first time under static loading then under fatigue loading. Two kinds of geometry were taken (Fig. 1): one for static testing (on a static testing machine) the other for fatigue testing (on a fatigue testing machine). The samples were obtained from plates made in an autoclave with a curing cycle of 1 h at  $80^\circ\text{C}$ , followed by 2 h at  $180^\circ\text{C}$  under a pressure of 4 bars. The plates were then cut out and machined under numerical control. The choice made it possible to rule out the occurrence of edge effects at the level of the tabs. The initial static strength  $\sigma_{ult}$  was about 160 MPa and the initial shearing modulus  $G_0$  was about 3400 MPa.

The static tests were carried out on a static testing

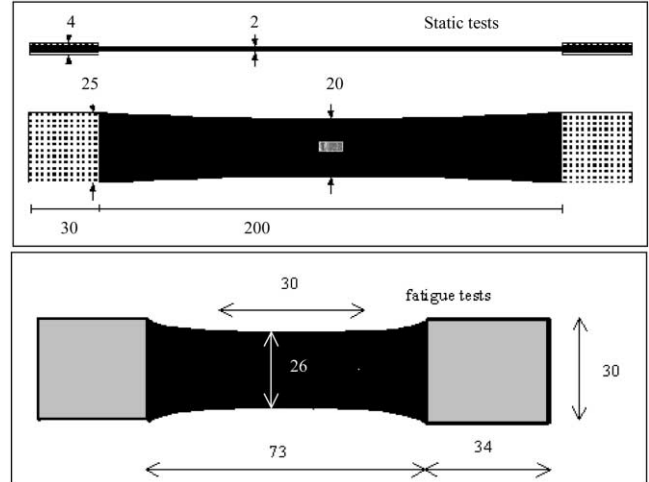


Fig. 1. Samples geometry (size in mm). Aluminium tabs.

machine on two kinds of laminates:  $[\pm 45]_{3s}$  and hybrid glass/carbon  $[0(\text{glass}),90_2(\text{carbon})]_s$ . These stacking sequences allow to identify separately shearing behaviour and transverse tension behaviour. In the hybrid laminate, the on-axis glass plies prevent brittle failure of  $90^\circ$  plies to appear too early. Glass fibres were chosen instead of carbon fibres because the first intra-laminar macro-crack of the carbon plies can be easily observed. The fatigue tests were carried out on a fatigue machine, with the stresses imposed at a frequency of 35 Hz (which was directly correlated with the oscillating load). In a first stage, the stress ratio (minimal stress over maximal stress) remains constant at 0,5 and the plastic strain evolution is not measured during fatigue loading. The dynamic and creep phenomena were not taken into account. The sample temperature was increased by approximately  $20^\circ$  at the end of the test; mechanical characteristics were assumed to be unaffected by this change.

The tests under strain control are now under way. The test method adopted for this purpose is a four point bending test, and the samples used are sandwich structures (a laminate with unidirectional plies forming the bottom flange, a honeycomb and a woven ply laminate at  $0^\circ$  forming the top flange). With this sandwich structure, it is possible to create an almost uniform state of strain in the unidirectional plies, and the woven plies are assumed to undergo almost no degradation. An advantage of the four point bending test is that it is possible to prescribe a compression load on the plies.

### 2.2. Experimental observations under static loading

A ply has different kinds of behaviour with respect to the direction loading (see Fig. 2):

- In the fibre direction the behaviour is elastic and brittle. No damage is observed before the fracture,

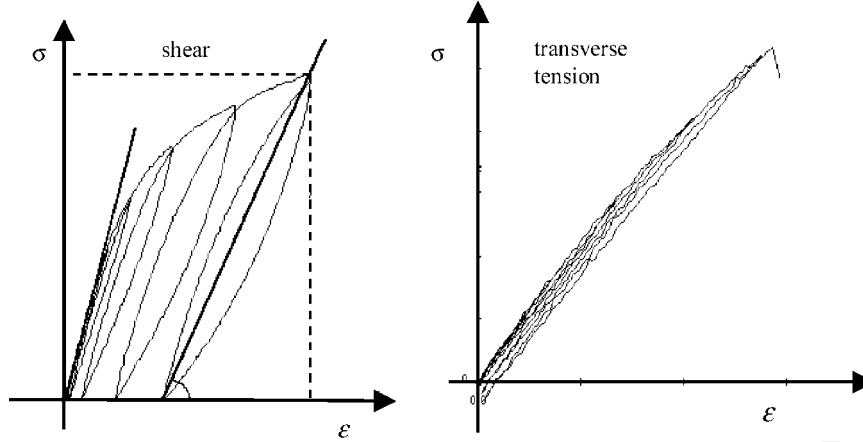


Fig. 2. Identification of shear and transverse tension behaviour.

- In shearing, which is obtained from a tension test on a  $[+45, -45]_s$  laminate, we can observe a non-linear behaviour: there are anelastic strains and during elastic unloadings we can observe a loss of rigidity (that is damage); the rupture of the laminate corresponds to a phenomena of structure instability.

In transverse tension, we observe a loss of rigidity due to damage; there is a phenomenon of brittle failure in transverse tension. On the tested material (G827/914) [11], the loss of rigidity in transverse tension was approximately 20%.

These experimental results obtained under static loading justify the existence of a stage of a diffuse damage before the occurrence of the first transverse rupture. The modelling that we develop in the next part is mainly based on this phenomenon: it exists a stage without any macro-cracks i.e. without any ply failure.

### 3. Modelling of the behaviour under static and fatigue loadings

#### 3.1. Damage mechanics of anisotropic materials

The model is based on the theory of damage mechanics, in which internal variables are used to describe the progressive loss of rigidity of the ply. It is assumed here that the rupture mode in the fibre direction is elastic and brittle and that it does not depend on the cyclic loading. Two scalar damage variables are introduced in order to describe the loss of rigidity under transverse tension and shear loading conditions. The in-plane transversal and shear moduli are modified under the assumption of a progressive damage associated to micro-cracks parallel to the fibres [11]. The development of these damage variables depends on the static and cyclic loadings, and they are coupled. The anelastic strains observed are

accounted for via a plastic-hardening model coupled with the damage.

Based on the thermodynamic formulas, we can write the density of the free energy, making the ‘plane-stress’ assumptions, in the following form:

$$\rho\Psi = \frac{1}{2} \left[ \frac{(\sigma_{11})^2}{E_1^0} - \frac{2\nu_{12}^0\sigma_{11}\sigma_{22}}{E_1^0} + \frac{\langle\sigma_{22}\rangle_+^2}{E_2^0(1-d')} + \frac{\langle\sigma_{22}\rangle_-^2}{E_2^0} + \frac{(\sigma_{12})^2}{2G_{12}^0(1-d)} \right] \quad (1)$$

where: subscripts 1 and 2 denote the fibre and transverse directions, respectively;  $E_1^0$ ,  $E_2^0$ ,  $G_{12}^0$  and  $\nu_{12}^0$  are the elastic coefficients of the ply;  $d$  and  $d'$  are the scalar-damage variables describing the loss of rigidity under shear and transverse tension loading, respectively;  $\nu_{12}$  is supposed to remain constant and thus  $\nu_{21}$  is function of  $d'$ :  $\nu_{21} = \nu_{12}^0(1-d')$ .

The transverse tension energy and compression energy are split in order to describe the unilateral feature resulting from the opening and closing of the micro-cracks. In the case of a transverse compression load, micro-cracks close up and thus the transverse direction behaviour remains undamaged. From this potential, the conjugated quantities associated with the stresses (i.e. the elastic strains) are defined as follows:

$$\varepsilon_{11}^e = \frac{\sigma_{11}}{E_1^0} - \frac{\nu_{12}^0\sigma_{22}}{E_1^0}; \varepsilon_{22}^e = \frac{\langle\sigma_{22}\rangle_+}{E_2^0(1-d')} + \frac{\langle\sigma_{22}\rangle_-}{E_2^0} - \frac{\nu_{12}^0\sigma_{11}}{E_1^0}; \varepsilon_{12}^e = \frac{\sigma_{12}}{2G_{12}^0(1-d)} \quad (2)$$

and the thermodynamic forces associated with the damage variables  $d$  and  $d'$  are obtained:

$$Y_d = \rho \frac{\partial \Psi}{\partial d} \Big|_{\sigma, d'} = \frac{\sigma_{12}^2}{2G_{12}^0(1-d)^2} \quad Y_{d'} = \rho \frac{\partial \Psi}{\partial d'} \Big|_{\sigma, d} = \frac{\langle\sigma_{22}\rangle_+^2}{E_2^0(1-d')^2} \quad (3)$$

The development of the damage depends on these associated forces. The ‘transverse tension/ shear’ coupling effect is taken into account, based on an equivalent associated force  $Y(t)$  which is defined from the maximum value observed throughout the loading history:

$$Y(t) = \sup_{\tau < t} (Y_d(\tau) + bY_{d'}(\tau)) \quad (4)$$

where  $b$  is a ‘transverse tension/shear’ coupling parameter.

### 3.2. Framework of cumulated damage

The development of the damage variables  $d$  and  $d'$  depends on the static and cyclic loadings involved. Here we take the cumulated damage: the total damage  $d$  is the result of damage  $d_s$ , named the ‘static damage’, associated with the static loading, superimposed on damage  $d_f$ , named ‘fatigue damage’, associated with the fatigue loading:

$$d = d_s + d_f \quad d' = d'_s + d'_f \quad (5)$$

where the damage variables  $d$  and  $d'$  ranges from 0 to 1. The development of the damage variables depends on the loading levels and the damage states. It should be recalled that in this study, the range of validity of the model is limited to the first intra-laminar macro-crack and that the delamination phenomena are not modelled.

### 3.3. Development of the ‘static damage’

In the case of the unidirectional plies under static loading, a first approximation of the damage development, which corresponds to a linear law with respect to the square root of the equivalent associated force  $Y$ , shows a good fit with the experimental data:

$$d_s = \frac{\langle \sqrt{Y} - \sqrt{Y_0} \rangle_+}{\sqrt{Y_c} - \sqrt{Y_0}} \quad \text{if } d < 1 \quad d'_s = b'd_s \quad \text{if } Y_{d'} < Y'_c \quad \text{else } d' = 1 \quad (6)$$

where the coefficients  $b'$  stand for the ratio between the transverse damage and the shear damage,  $\sqrt{Y_0}$  and  $\sqrt{Y_c}$  correspond to the threshold and the critical value of the development of  $d_s$ , respectively, and  $Y_{d'}$  is a parameter which defines the ultimate force in the transverse direction (see Fig. 3). The parameter values are obtained by

identification in static tests. The rupture criteria depend on the direction: brittle in the fibre direction, brittle fracture after damage under transverse tension loading and rupture as the result of instability under shear loading conditions.

### 3.4. Development of the ‘fatigue damage’

The development of the ‘fatigue damage’ depends on the loading occurring during a cycle, which may evolve with time and depends on the damage state. A simple fatigue law (similar to Kachanov law [12]) which provides the development of the fatigue damage can be written in the following form:

$$\frac{\partial d_f}{\partial N} = g * \langle \sqrt{Y_f} - \sqrt{Y_{of}} \rangle_+ \quad \text{with } Y_f(t) = \sup_{\tau \in \text{cycle}(t)} (Y_d(\tau) + bY_{d'}(\tau)) \quad (7)$$

$$d'_f = b'd_f \quad \text{if } Y_{d'} < Y'_c \quad \text{else } d' = 1$$

where the coefficient  $g$  is taken to be constant at the moment and  $Y_f(t)$  is the maximum equivalent force during a cycle. New experimental tests have to be done to defined dependence of the coefficient  $g$  on the loading ratio  $R$  (ratio of the minimum equivalent force to the maximum equivalent force during a cycle). The parameter  $\sqrt{Y_{of}}$  defines the endurance threshold, i.e., the loading level below which no development of the ‘fatigue damage’ occurs.

Note that during fatigue loading, the development of the fatigue damage leads to an increase in the cumulated damage, and may cause the static damage to evolve because of the changes in the equivalent associated force  $Y$ . Consequently, if a new static load is imposed after this fatigue loading, the damage evolution will stay continuous.

### 3.5. Modelling anelastic strains

After a loading process has taken place in a laminate, residual strains can be observed. These strains can be linked to the friction occurring between the fibres and the matrix due to the damage, but they can also be generated by the plasticity of the matrix. To describe them, an isotropic hardening model was developed and it is

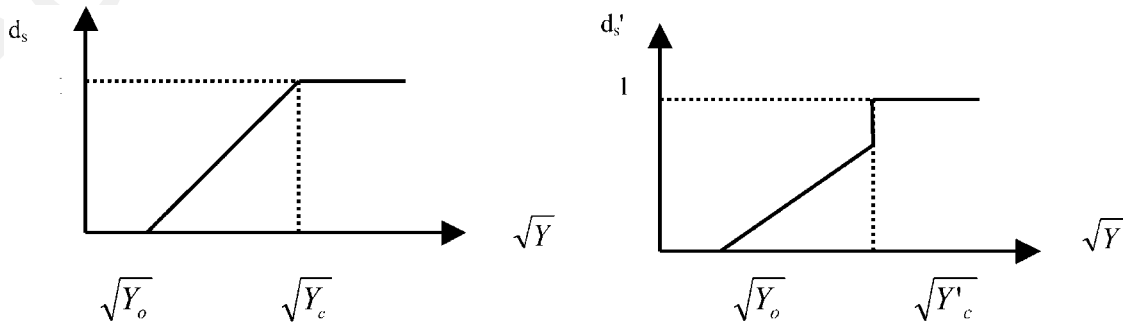


Fig. 3. Evolution of damage variables under static loading. (Left) shear damage variable; (right) transverse tension damage variable.

coupled with damage via effective quantities [11] based on the equivalence of plasticity dissipation  $\Phi_p$ :

$$\Phi_p = Tr(\sigma \dot{\epsilon}_p) = Tr(\tilde{\sigma} \dot{\tilde{\epsilon}}_p) \quad (8)$$

where the effective stresses are defined as follows:

$$\tilde{\sigma}_{11} = \sigma_{11}; \quad \tilde{\sigma}_{22} = \frac{\langle \sigma_{22} \rangle_+}{1-d'} + \langle \sigma_{22} \rangle_-; \quad \tilde{\sigma}_{12} = \frac{\sigma_{12}}{1-d} \quad (9)$$

and the effective strains are defined as follows:

$$\begin{aligned} \dot{\tilde{\epsilon}}_{11} &= \dot{\epsilon}_{11}^p; \quad \dot{\tilde{\epsilon}}_{22} = \dot{\epsilon}_{22}^p \left( \frac{\langle \sigma_{22} \rangle_+}{\sigma_{22}} (1-d') + \frac{\langle \sigma_{22} \rangle_-}{\sigma_{22}} \right); \quad \dot{\tilde{\epsilon}}_{12} \\ &= \dot{\epsilon}_{12}^p (1-d) \end{aligned} \quad (10)$$

In the fibre direction, it is assumed that there is no plastic strain  $\dot{\epsilon}_{11}^p = 0$  and that the stress  $\sigma_{11}$  has no effect on the plasticity. The elastic field is defined by the function  $f$ :

$$f = (\tilde{\sigma}_{12}^2 + a^2 \tilde{\sigma}_{22}^2)^{1/2} - R(p) - R_0 \quad (11)$$

where  $p$  is the cumulated plasticity index,  $R_0$  and  $a$  are coefficients and  $R(p)$  is the hardening function such that:

$$R(p) = K p^\alpha \quad (12)$$

where  $K$  is the power law coefficient and  $\alpha$  is the power law exponent. The hardening law is assumed to be identical under both static and fatigue conditions. Other tests are going to be carried out to check this assumption. Note that during fatigue loading under stress control, the development of the fatigue damage leads to an increase in the cumulated damage, and the effective stress increase so plasticity evolve.

### 3.6. Simulation of the behaviour up to rupture of the first ply

All these relations provide the evolution of the damage variable and the endurance curve. Here we give an example of a simulation in the case of a laminate  $[\pm 45^\circ]_{ns}$  (see Figs. 4–6). This stacking sequence was chosen with an aim of creating in each ply a state of almost pure shear stress: the transverse stress  $\sigma_{22}$  is negligible in comparison with the shear stress  $\sigma_{12}$ .

In a first case, the development of the state of the plies is studied when a constant stress is imposed. Fig. 4 gives the simulated evolution of the shear damage versus the number of cycles on the left, and versus  $\sqrt{Y}$  on the right. The total damage is split up into the static damage  $d_s$  and the fatigue damage  $d_f$ . One can note that the static damage increases linearly as a function of  $\sqrt{Y}$  during the first cycle (following the ‘static damage’ model) and that it continues to evolve during the fatigue loading. In this case of ‘imposed stresses’, all the variables ( $d_s$ ,  $d_f$ ,  $Y$ ,  $\epsilon_e$ ,  $\epsilon_p$ , ...) evolve in a coupled way. Fig. 5 gives the simulated life curve, i.e. the loading (maximum stress) versus the number of cycles to failure. In the case of a  $[\pm 45^\circ]_{ns}$ , complete failure of the structure is taken to have occurred when the structure has reached a state of instability (in terms of the strain localisation, i.e. a horizontal asymptote on the curve stress/strain). The figure on the right-hand side (Fig. 5) corresponds to the loading versus the logarithm of the number of cycles. The endurance curve is Z-shaped.

In a second case, the evolution of the state of the plies is studied when constant strains are imposed. Fig. 6 gives the simulated evolution of the shearing damage

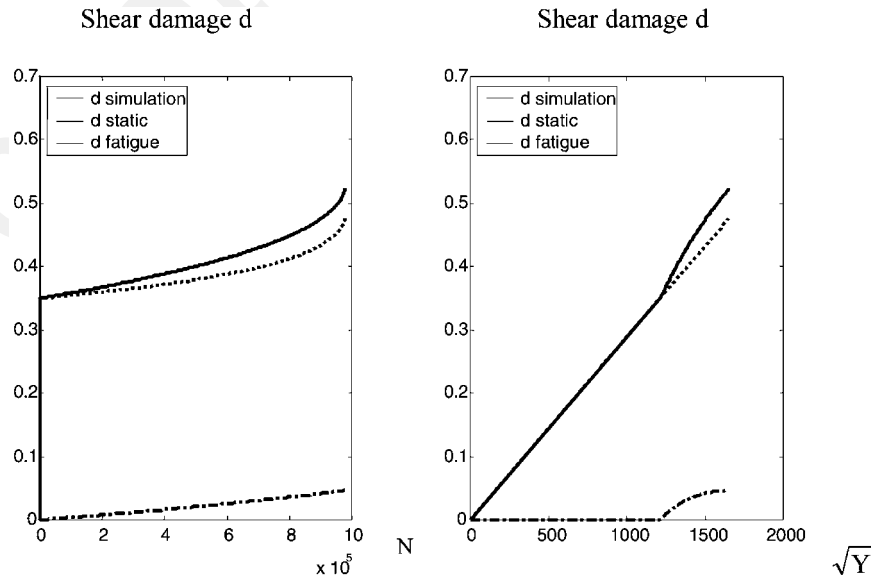


Fig. 4. Simulation of damage evolution under stress control. (Left) shear damage variable evolution versus number of cycles; (right) shear damage variable evolution versus square root of  $Y$ .

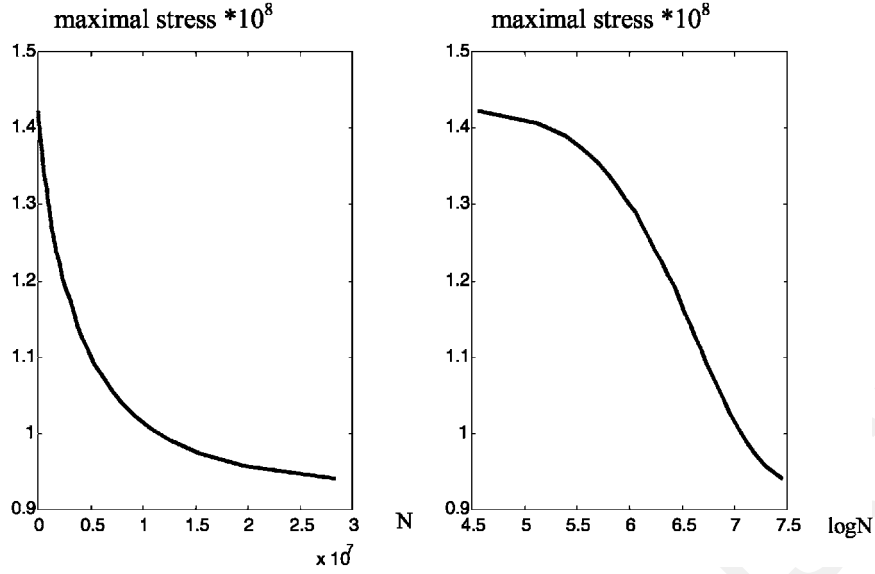


Fig. 5. Life curve i.e. maximum stress versus number of cycles at failure. (Left) linear scale of number of cycles; (right) logarithmic scale of number of cycles.

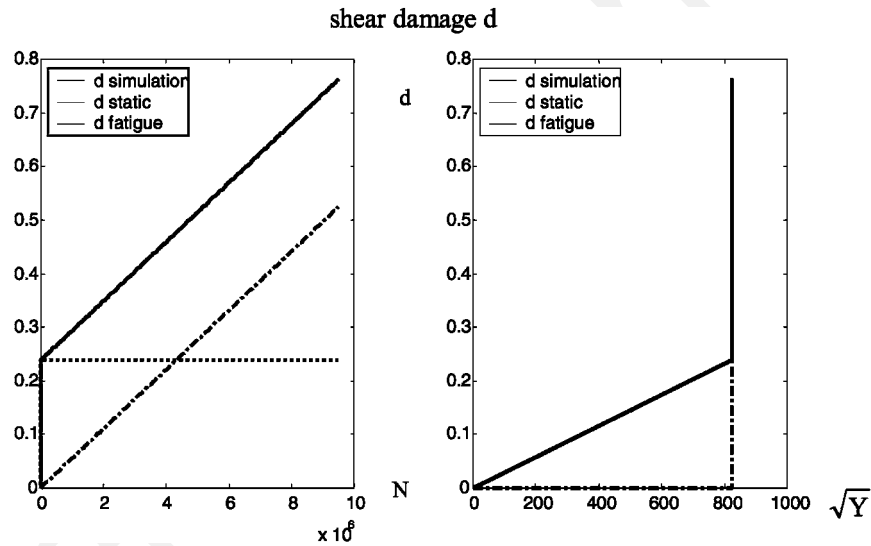


Fig. 6. Simulation of damage evolution under strain control. (Left) Evolution of shear damage variable versus number of cycles; (right) Evolution of shear damage variable versus root of  $Y$ .

versus the number of cycles on the left and versus  $\sqrt{Y}$  on the right. The same static/fatigue decomposition of the damage was carried out and it was noted that the static damage does not evolve when the number of cycles increases. In this particular case, the associated force  $Y$  remains constant and the imposed total strain, the elastic strain and the anelastic strain are all constant. Based on our model, it can be stated that during the 'imposed strains' fatigue loading, fatigue damage is the only variable among all which evolves. This property makes this test particularly useful for identifying the fatigue parameters.

Under both kinds of loading (imposed stresses or strains), the model makes it possible to know the state of

the material at any moment in its history, i.e., it gives both the state of damage and the state of plasticity reached.

#### 4. Comparison modelling/testing under fatigue loading

The experimental and simulated results (Figs. 7 and 8) were compared after identifying the coefficients. They showed satisfactory agreement in view of the current state of development of the experimental procedure and of precision of the model. The rupture of the samples [ $\pm 45^\circ$ ]<sub>ns</sub> was obtained by introducing a structure insta-

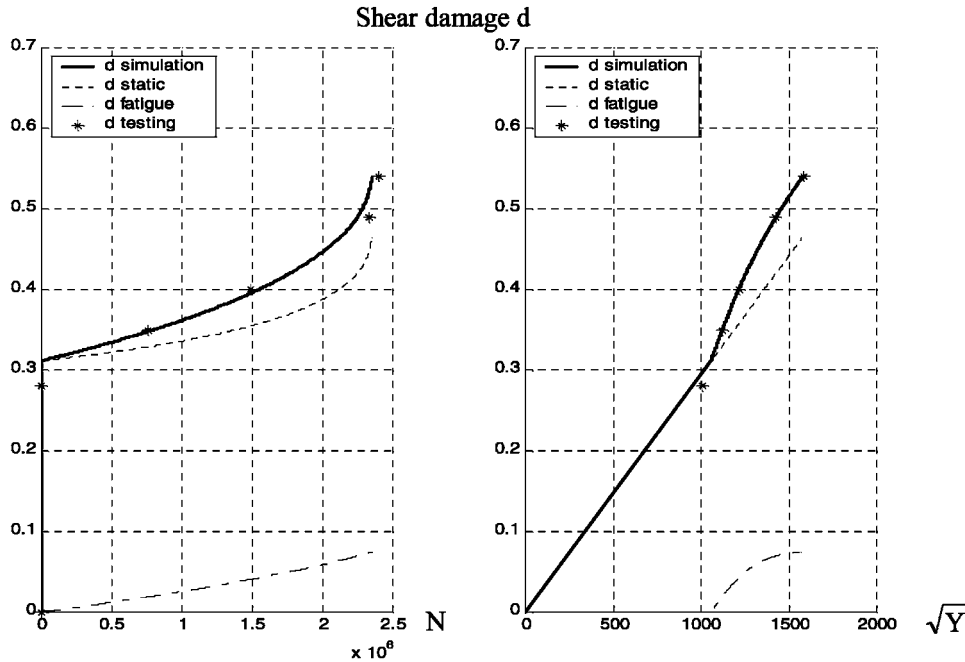


Fig. 7. Simulation of damage evolution  $\sigma_{\max}=120$  MPa  $R=0.5$ . Comparison model/test.

bility condition. Under static loading, this condition corresponds to a damage value  $d=0.5$ , although under fatigue loading, this value can be greater. Fig. 8 shows the endurance curve obtained on the basis of the first tests: normalised stress (i.e. maximal stress over ultimate static stress) is plotted versus log of number of cycles at failure. The endurance limit (the maximal stress value at which the life of the structure will be greater than  $2 \cdot 10^7$  cycles and the fatigue damage will be zero) has been found to be approximately 90 MPa. The number of experiments carried out so far (under both identical and varied test conditions) is not large enough to be able to provide quantitative information about the material

tested. However, we have obtained some useful qualitative information.

### 5. Conclusions

The results of this modelling and experimental study are fairly conclusive, since the experimental data obtained so far are in good agreement with the model. In addition, they confirm the validity of using a combined modelling and experimental approach to the physical phenomena investigated here, namely micro-crack damage and first ply failure; this approach is particularly adapted for an industrial context where safety is the major constraint. On the other hand, this study is just the first part of a larger experimental project, in which it is proposed to extend this model and to ensure that it is reliable. It should eventually be possible with this model not only to predict the number of cycles required to produce first ply rupture, but also, to determine the state of the material at any moment. The next step will therefore consist of integrating this behaviour into a finite-element code in order to simulate the behaviour of a laminated composite structure under complex (static and/or fatigue) loading conditions.

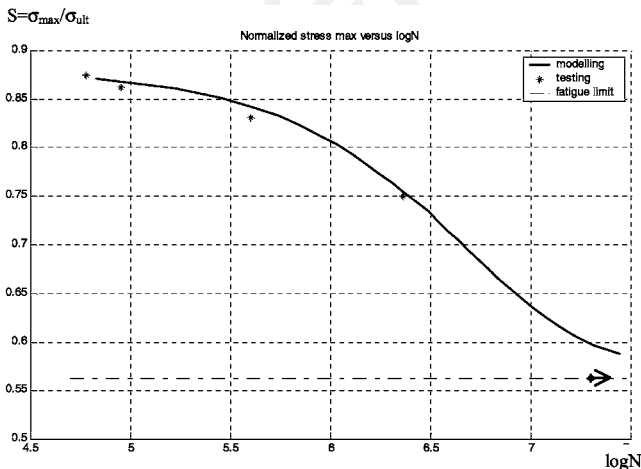


Fig. 8. S–N curve i.e. maximum normalised stress versus log of number of cycles at failure. Comparison model/test.

### References

[1] Reifsnider K. Durability and damage tolerance of fibrous composite systems. In: Peters St, editor. Handbook of composites, vol. 35. Chapman & Hall, 1998:794–809.

- [2] Talreja R. Fatigue of composite materials: damage mechanisms and fatigue-life diagrams. *Proc R Soc Lond A* 1981;378:461–75.
- [3] Wang ASD. Strength, failure, and fatigue analysis of laminates. In: *Engineered materials handbook*, ASM, vol. 1, 1987:236–51.
- [4] Jen M-HR, Lee C-H. Strength and life in thermoplastic composite laminates under static and fatigue loads. *Int J Fat* 1998;19:605–15.
- [5] Shokrieh M-M, Lessard L-B. Multiaxial fatigue behaviour of unidirectional plies based on uniaxial fatigue experiments. *Int J Fat* 1997;20:201–17.
- [6] Gao Z. A cumulative damage model for fatigue life of composite laminates. *J Reinf Plast Comp* 1994;13:128–41.
- [7] Ladeveze P, Le Dantec E. Damage modelling of the elementary ply for laminates composites. *Comp Sci Technol* 1992;43(3):257–68.
- [8] Thionnet A, Renard J. Modelling unilateral effect in strongly anisotropic materials by the introduction of the loading mode in damage mechanics. *Int J Solids Struct* 1999;36:4269–87.
- [9] Caron JF, Erlacher A. Modelling of fatigue microcracking kinetics in crossply composites and experimental validation. *Comp Sci Technol* 1998;59(9):1349–59.
- [10] Sims DF, Brogdon VH. Fatigue behaviour of composites under different loading modes. In: *Fatigue of filamentary composite materials*, ASTM STP636, 1977:185–205.
- [11] Charles JP, Fatichi R, Hochard C, Mazerolle F. Experimental analysis of the transverse behaviour of unidirectional carbon/epoxy plies, *JNC11*. AMAC, 1998;3:1029–38.
- [12] Kachanov LM. Time of the rupture process creep conditions. *Izv Akad Nauk S.S.R. Otd Tech Nauk* 1958;8:26–31.